Detection and Cancellation of Motion Artifact in fNIRS Device Using Kalman Filter and Discrete Fourier Transform

Kensuke Uesugi
Graduate School of Science and Engineering
Doshisha University
Kyotanabe, Japan
e-mail: uesugi0410@gmail.com

Masafumi Hashimoto, Kazuhiko Takahashi
Faculty of Science and Engineering
Doshisha University
Kyotanabe, Japan
e-mail: {mhashimo, katakaha}@mail.doshisha.ac.jp

*Abstract***—This paper presents a method for detecting and cancelling motion artifacts related to standing and walking in a functional near-infrared spectroscopy (fNIRS) signal. Our fNIRS device has 22 channels. The motionless fNIRS signal from each channel is represented by a fourth-order autoregressive (AR) model, and the related parameters are estimated based on the motionless fNIRS signal using the Yule Walker equation. The motion artifacts included in the fNIRS signal are cancelled using the Kalman filter constructed from the AR model. However, the cancellation may be insufficient when the motion artifacts are strong. To determine in which fNIRS channels the motion artifacts are cancelled insufficiently, we apply a measurement prediction error related to the Kalman filter and a discrete Fourier transform. The brain activity of the user is then recognized from those fNIRS channels in which the motion artifacts are cancelled sufficiently. To evaluate the proposed method, a mobile robot is controlled using an fNIRS devise as worn by 10 subjects while standing, walking, or sitting. The experimental results show the performance of the proposed method.**

Keywords-fNIRS; Motion artifact; Detection and cancellation; AR model; Kalman filter; Discrete Fourier transform

I. INTRODUCTION

Human brain activity is being measured in fields, such as automobile driving, rehabilitation, and computer interfaces [1][2][3]. Various devices have been developed for measuring human brain activity, such as electroencephalography (EEG), functional magnetic resonance imaging (fMRI), and functional near-infrared spectroscopy (fNIRS).

fNIRS devices measure the brain activity from changes in the hemoglobin concentration (fNIRS signals). This has the advantage of being less restrictive compared with EEG or fMRI devices [4] [5]. However, the disadvantage with fNIRS devices is that they can be disturbed by artifacts due to body movement, fatigue, and anxiety, for example [5]. Such artifacts have to be removed before the brain activity can be evaluated correctly using an fNIRS signal.

Many methods have been proposed for removing motion artifacts from an fNIRS signal [6][7][8]. Cooper et al. [6] proposed a method that removes motion artifacts using spline interpolation, wavelet analysis, Kalman filter, or principal component analysis. Izzetoglu et al. [9] proposed a method that identifies a motionless fNIRS signal using an autoregressive (AR) model, and then constructed an AR model-based Kalman filter to remove the motion artifacts. Admian et al. [10] applied an autoregressive moving-average (ARMA) model to identify a motionless fNIRS signal.

However, the aforementioned methods removed only motion artifacts due to head motion while sitting. Such methods are expected to be ineffective for large motion artifacts caused by body movements, such as standing or walking. Hiroyasu et al. [11] attached an accelerometer to the head. Because acceleration and the fNIRS signal are largely correlated during head motion, they were able to remove the motion artifacts by using an independent component analysis. This method enables motion artifacts to be removed easily, however, it required an additional sensor other than the fNIRS device.

In this paper, we consider motion artifacts that occur in the fNIRS signal during standing and walking. We propose a method of detecting and cancelling such motion artifacts using the Kalman Filter and the discrete Fourier transform. We verify our proposed method experimentally with a mobile robot controlled by human brain activity.

The remainder of this paper is organized as follows. In Section II, we give an overview of our experimental system. In Section III, we present our method for detecting and removing motion artifacts from an fNIRS signal. In Section IV, we describe a method for controlling a mobile robot via human brain activity. In Section V, we conduct experiments on mobile-robot control to verify the proposed method, followed by conclusions in Section VI.

 ISBN: 978-1-61208-621-7

II. Experimental System

Figure 1 shows the configuration of our experimental system. The fNIRS signal obtained from the fNIRS device is transmitted to a control personal computer (PC) via a wireless LAN and a data-capture PC. The control PC recognizes the brain activity (as either active or inactive) and then sends a command (either run or stop) to the mobile robot according to the brain activity.

As shown in Figure 2, the fNIRS device has 22 output channels, each of which measures an fNIRS signal in the human prefrontal cortex every 0.2 s using near-infrared light (700–900 nm). The fNIRS signal comprises an oxygenated hemoglobin (OxyHb) concentration and a deoxygenated hemoglobin (DeoxyHb) concentration. When the brain is active, OxyHb increases and DeoxyHb decreases. In this paper, we use only the OxyHb concentration as the fNIRS signal.

III. Method for Detecting and Cancelling Motion Artifacts

A. Reducing Motion Artifacts Using Kalman Filter

When body movement (e.g., jaw, eyes (blinking), and head) occurs, contact between the fNIRS device and the scalp becomes unstable and thus motion artifacts appear in the fNIRS signals. Such motion artifacts cause the brain activity based on the fNIRS signal to be recognized incorrectly, and so need to be removed.

We use the following fourth-order AR model to reduce the motion artifacts in an fNIRS signal [8]:

$$x_k = a_3 x_{k-1} + a_2 x_{k-2} + a_1 x_{k-3} + a_0 x_{k-4} + w_k \tag{1}$$

where k–i (i = 0–4) denotes a time step, x_{k-i} denotes an fNIRS signal that contains no motion artifacts, and a_i (j = 0–3) denotes a coefficient. w_k denotes the model error, which is assumed to be a normal white-noise sequence with zero mean and variance q. We set $q = 5.0 \times 10^{-4}$ (mM × mm)^2 in the experiments in Section V.

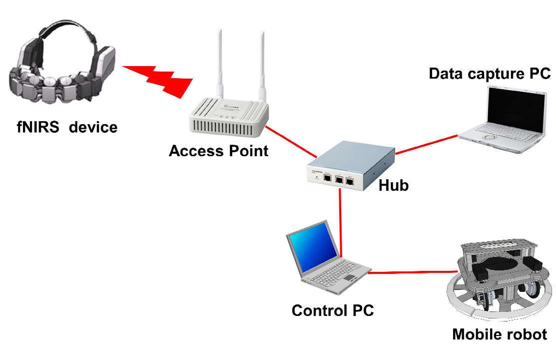

Figure 1. Overview of experimental system.

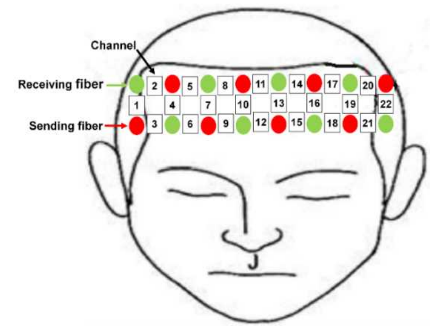

Figure 2. Output channels of fNIRS device.

We obtain the values of coefficient a_i (j = 0–3) from the fNIRS signal measured while sitting and hence including no motion artifacts. The following state equation is obtained from (1):

$$\begin{aligned} \boldsymbol{x}_k &= \boldsymbol{A}\boldsymbol{x}_{k-1} + \boldsymbol{B}w_k \\ &= \begin{pmatrix} a_3 & a_2 & a_1 & a_0 \\ 1 & 0 & 0 & 0 \\ 0 & 1 & 0 & 0 \\ 0 & 0 & 1 & 0 \end{pmatrix} \boldsymbol{x}_{k-1} + \begin{pmatrix} 1 \\ 0 \\ 0 \\ 0 \end{pmatrix} w_k \end{aligned} \tag{2}$$

where $\boldsymbol{x}_k = \left(x_k \quad x_{k-1} \quad x_{k-2} \quad x_{k-3}\right)^T$.

The measurement equation is given by

$$\begin{aligned} z_k &= \boldsymbol{H}\boldsymbol{x}_k + v_k \\ &= \left(1 \quad 0 \quad 0 \quad 0\right)\boldsymbol{x}_k + v_k \end{aligned} \tag{3}$$

where z_k denotes the fNIRS signal that includes motion artifacts in the current time step k. v_k denotes the measurement noise, which is assumed to be normal white-noise sequence with zero mean and variance r. We set $r = 1.0 \times 10^{-5}$ (mM × mm)^2 in the experiments in Section V.

When we apply the Kalman filter [12] based on (2) and (3), the estimate $\hat{\boldsymbol{x}}_k$ and its associated covariance $\boldsymbol{P}_k$ for an fNIRS signal that does not contain motion artifacts can be obtained from the following algorithms:

- Prediction algorithm

$$\begin{cases} \hat{\boldsymbol{x}}_{k/k-1} = \boldsymbol{A}\hat{\boldsymbol{x}}_{k-1} \\ \boldsymbol{P}_{k/k-1} = \boldsymbol{A}\boldsymbol{P}_{k-1}\boldsymbol{A}^T + \boldsymbol{B}\boldsymbol{B}^T q \end{cases} \tag{4}$$

- Estimation algorithm

$$\begin{cases} \hat{\boldsymbol{x}}_k = \hat{\boldsymbol{x}}_{k/k-1} + \boldsymbol{K}_k (z_k - \boldsymbol{H}\hat{\boldsymbol{x}}_{k/k-1}) \\ \boldsymbol{P}_k = \boldsymbol{P}_{k/k-1} - \boldsymbol{K}_k \boldsymbol{H}\boldsymbol{P}_{k/k-1} \end{cases} \tag{5}$$

where $\boldsymbol{K}_k = \boldsymbol{P}_{k/k-1}\boldsymbol{H}^T / S_{k/k-1}$ and $S_{k/k-1} = \boldsymbol{H}\boldsymbol{P}_{k/k-1}\boldsymbol{H}^T + r$.

ISBN: 978-1-61208-621-7

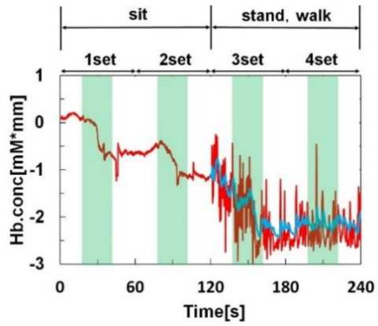

Figure 3 fNIRS (red) and efNIRS (blue) signals.

It should be noted that the coefficient estimation for the AR model and the Kalman-filter-based estimation for the fNIRS signal are performed in every channel of the fNIRS device.

Figure 3 shows an example of fNIRS signal (red lines) with and without motion artifacts. The subject wearing the fNIRS device remains seated for sets 1 and 2 and then stands up at the start of set 3 and walks until the end of set 4. During the task, the subject alternates between concentrating on moving the mobile robot (in the green areas in Figure 3) and not (in the white area). One set of 60 s comprises 15 s of rest prior to executing the task (pre-rest), 30 s of task activity, and then 15 s of rest (post-rest).

As shown in Figure 3, no motion artifacts appear in the fNIRS signal while sitting (sets 1 and 2), whereas motion artifacts contain while walking (sets 3 and 4). We estimate the AR-model coefficients at the end of set 2 using the Yule Walker equation [13] based on the fNIRS signal without motion artifacts during sitting (sets 1 and 2). We then apply the Kalman filter based on (4) and (5) and obtain an estimated fNIRS signal (hereinafter referred to as the efNIRS, blue line in Figure 3) from which motion artifacts have been removed. It is clear from this that the AR model can reduce the motion artifacts caused by walking.

B. Detecting and Removing Motion Artifacts

Sufficiently large motion artifacts in the fNIRS signal cannot be removed effectively even by applying the Kalman filter. Therefore, we execute the following process to identify whether the brain is in a state of activity or inactivity.

(a) Determine whether the fNIRS signal contains large motion artifacts;

(b) If so, determine whether they have been removed from the efNIRS signal sufficiently by the Kalman filter.

To achieve process (a), we use the measurement prediction error that is obtained using the Kalman filter. To achieve process (b), we use a discrete Fourier transform to obtain the power spectrum of the efNIRS signal.

The measurement prediction error $\tilde{z}_k$ can be defined as

$$\tilde{z}_k = z_k - \boldsymbol{H}\hat{\boldsymbol{x}}_{k/k-1} \tag{6}$$

where z_k denotes the fNIRS signal measurement, and $\hat{\boldsymbol{x}}_{k/k-1}$ denotes the fNIRS signal prediction obtained by the Kalman prediction algorithm given by (4).

We set the threshold value for the measurement prediction error as 0.4 from a preliminary experiment. If $|\tilde{z}_k| < 0.4$, we deem the fNIRS signal not to include large motion artifacts, and we use its estimate to recognize the brain activity. In contrast, if $|\tilde{z}_k| \geq 0.4$, we deem the fNIRS signals to include large motion artifacts, whereupon process (b) is applied.

To achieve process (b), we use the power spectrum PS of the efNIRS signal obtained by a discrete Fourier transform. We set the frequency and threshold values for the PS as 0.07 Hz and 2.0×10^{-4}, respectively, which were obtained from a preliminary experiment. If $PS < 2.0 \times 10^{-4}$ for a frequency of 0.07 Hz or greater, we deem large artifacts to have been removed sufficiently from the efNIRS signal, whereupon it is used to recognize the brain activity.

In contrast, if $PS \geq 2.0 \times 10^{-4}$ for a frequency of 0.07 Hz or greater , we deem large motion artifacts to be still present in the efNIRS signal, and we do not use the efNIRS signal to recognize the brain activity. For the discrete Fourier transform, we use 512 measurements and a Hamming window function.

IV. CONTROL METHOD FOR MOBILE ROBOT USING EFNIRS SIGNAL

We will conduct experiments on controlling a mobile robot (moving or stopping) in the following section to evaluate the proposed method. In this section, we describe the control method.

Any channel, whose output includes large motion artifacts, is not used for recognizing the brain activity. We perform this process for all 22 channels of the fNIRS device. Two appropriate output channels are selected from those that can be used to recognize the brain activity. Their efNIRS signals are used to recognize the brain activity and to control the robot. We refer to these two selected output channels as the control channels.

If channels that output a small fNIRS signal are used as the control channels, it is difficult to recognize the brain activity accurately. To use channels with high levels of brain activity as the control channels, firstly, we calculate two average values for the efNIRS signal, namely the average resting value in the rest section and the average task value in the task section. We obtain the difference between these average values and then use the two channels with the largest difference as the control channels.

Saika et al. [14] proposed a distance-type fuzzy reasoning method to recognize the brain activity from an fNIRS signal. In their study, subjects wore the fNIRS device while sitting, so that motion artifacts did not occur. In our study, we recognize the brain activity by applying the distance-type fuzzy reasoning method to the efNIRS signal containing motion artifacts. We outline this method below; further details can be found in [14][15].

The Kalman filter is used to estimate the output fNIRS signals of the control channels. Because an fNIRS signal would increases in the presence of brain activity, we introduce following three rules for robot control, in which the fluctuation in the efNIRS signal is used as the antecedent part and the switching of the robot control signals (output signals) as the consequent part:

・Rule 1: If the efNIRS signal increases compared with the previous state, turn the control signals on;

・Rule 2: If the efNIRS signal changes minimally or not at all compared with the previous state, maintain the current control signals;

・Rule 3: If the efNIRS signal decreases compared with the previous state, turn the control signals off.

Also, to compare the efNIRS signal in the current time step with that in the previous time step, we use the efNIRS signal from five time frames, namely the current one and those 0.4 s, 0.8 s, 1.2 s, and 3.0 s previously.

The distance-type fuzzy reasoning method is used to recognize the brain activity in each of the two control channels. Thus, when the output results from these two channels coincide, they are sent to the robot as the output signals. When the output results are different, the output signals are turned off.

V. Experimental Results

To verify the proposed method, we compare the results of robot control in two cases: using the efNIRS signal obtained by the proposed method and using the original fNIRS signal. The subjects are nine men and one woman in their 20’s, to whom we explain the experiment outline and from whom we acquire informed consent prior to the experiments.

Figure 4 shows the flow of the experimental process. Each experiment comprises 10 sets, each of which consists of 15 s of pre-rest, 30 s of task, and 15 s of post-rest (a total of 60 s). Each subject performs the experiment twice. The subjects are instructed to concentrate during the task time (i.e., focus on moving the robot) and rest during the rest time.

During the preparation stage shown in Figure 4, the subjects perform tasks and rest while sitting without controlling the robot. During the robot-controlling stage, they control the robot while standing, sitting, and walking. The subjects avoid moving their heads while transitioning from sitting to standing and vice versa. They also walk at a normal speed. In the experiments, the robot moves if the brain activity is recognized as being active, and it stops if the brain activity is recognized as being inactive.

To verify the efficacy of the proposed method, the robot is controlled using the proposed method during sets 3–5, 9, and 10. In contrast, the robot is controlled using the original fNIRS signal during sets 6–8. It should be noted that the subjects do not know during which sets the proposed method will be applied.

The AR-model coefficients are estimated based on the fNIRS signal acquired during the preparation stage (sets 1 and 2), and two control channels are selected at the end of set 2. In sets 3–5, the robot is controlled by the efNIRS signals of the selected control channels. Because the robot is controlled using the original fNIRS signal during sets 6–8, we select two control channels at the end of set 5 using the original fNIRS signal during set 5.

Because the subjects become fatigued as the experiment progresses, the control channels and AR-model coefficient estimates acquired during sets 1 and 2 tend to differ from those found during sets 9 and 10. To address this problem, we estimate the AR-model coefficients during the robot control and again select two channels at the end of set 8. In sets 9 and 10, the robot is controlled by the efNIRS signals of the selected control channels.

As an example, we show the experimental results for subject “A”. Channels 1–4 and 20–22 in the fNIRS device are not used because of their relatively low S/N ratios; therefore, the experiment is performed using only the remaining 15 channels. The proposed method is used to select the control channels: channels 9 and 12 during sets 3–5, channels 7 and 12 during sets 6–8, and channels 6 and 12 during sets 9 and 10.

Figure 5 shows the results obtained using the proposed method during sets 3–5 (120–300 s). Figure 5 (a) shows the output signals for channel 12 of the fNIRS device, and Figure 5 (b) shows the corresponding robot control signals. The efNIRS signals are also shown in Figure 5 (b). The robot moves while the control signal output is “ON”, and it stops while the control signal output is “OFF”.

We can see from these figures that the robot is controlled in accordance with the changes in the efNIRS signal. The control output signals turn on when the estimate shows an increasing trend, and turn off when that trend is a

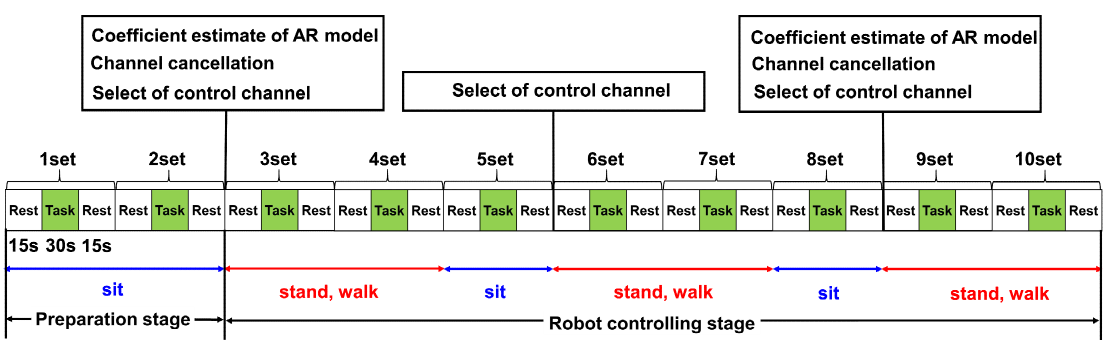

Figure 4. Experimental flow.

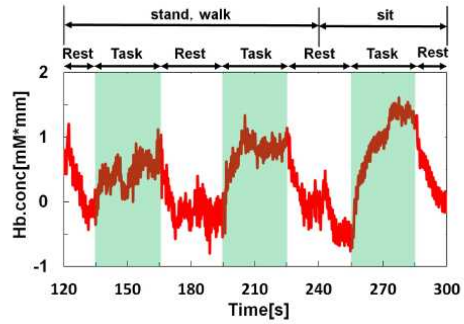

(a) fNIRS signal (12ch).

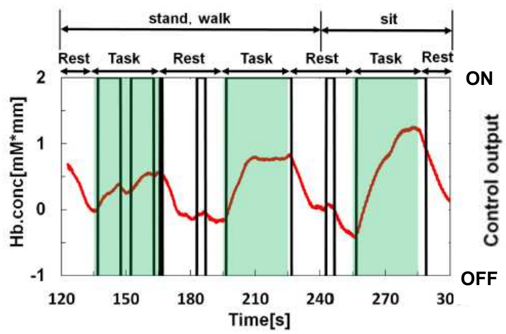

(b) efNIRS signal and control output (12ch).

Figure 5. fNIRS and efNIRS signals and control output by the proposed method during sets 3–5.

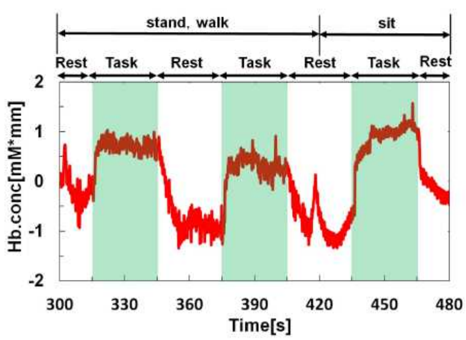

(a) fNIRS signal (12ch).

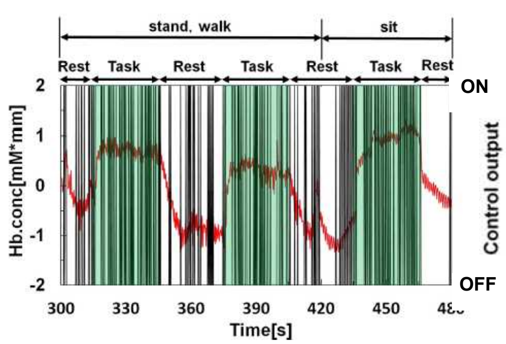

(b) fNIRS signal and control output (12ch)

Figure 6. fNIRS signal and control output without the proposed method during sets 6–8.

decreasing one. However, the output signals turn on at 180–190 s and 240–250 s because the estimates then exhibit extremely small increasing trends during the rest time.

Figure 6 shows the results without the proposed method during sets 6–8 (300–480 s). Figure 6 (a) shows the output signals for channel 12 of the fNIRS device, and Figure 6 (b) shows the corresponding robot control signals. The fNIRS signals are also shown in Figure 6 (b). Because the fNIRS signals contained motion artifacts are fluctuated over short periods of time, the robot-control output signals are switched frequently and repeatedly between on and off. Therefore, the robot cannot be controlled correctly.

To compare quantitatively the recognition performance with and without the proposed method, we calculate the average recognition success rate of the brain activity for the 10 subjects. The average recognition success rate indicates the success rate for controlling the robot and is defined as follows:

$$\text{Average recognition success rate} = \frac{1}{2}(\text{Rest recognition success rate} + \text{Task recognition success rate}) \quad (7)$$

where the rest (task) recognition success rate is defined as

$$\text{Rest recognition success rate} = \frac{\text{Time while control signals are off during rest time}}{\text{Rest time}} \quad (8)$$

$$\text{Task recognition success rate} = \frac{\text{Time while control signals are on during task time}}{\text{Task time}} \quad (9)$$

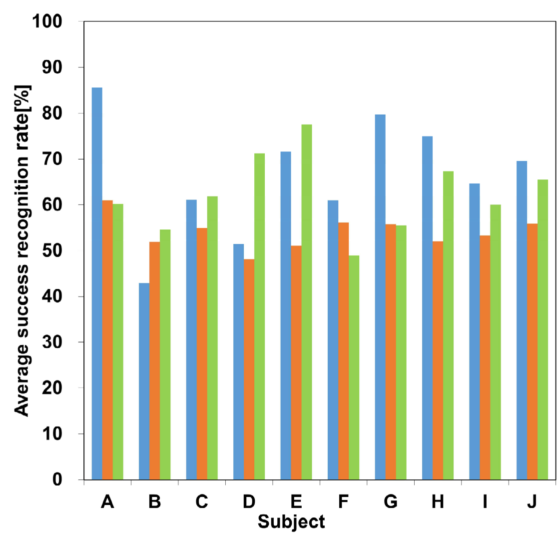

Figure 7. Average success recognition rate of 10 subjects.

Figure 7 shows the results. Blue bar indicates the result by the proposed method (sets 3–5). Green bar indicates the result by the proposed method (sets 9 and 10). Orange bar indicates the result without the proposed method (sets 6–8).

When using the proposed method, 8 of the 10 subjects have an average recognition success rate of 60% or greater during sets 3–5, and 7 of the 10 subjects have an average recognition success rate of 60% or greater during sets 9 and 10. In contrast, when the proposed method is not used, only one of the 10 subjects has an average recognition success rate of 60% or greater during sets 6–8. When the proposed method is used, the average recognition success rate for the 10 subjects is 66.3% during sets 3–5 and 62.2% during sets 9 and 10. In contrast, when the proposed method is not used, it is only 54% during sets 6–8.

VI. CONCLUSIONS

In this paper, we proposed a method for detecting and cancelling motion artifacts due to standing and walking in the fNIRS signals acquired by a multi-channel fNIRS device.

We identified the motionless fNIRS signal (while sitting) using a fourth-order AR model, and then reduced the motion artifacts due to standing and walking in the fNIRS signals using an AR-model-based Kalman filter. We used the measurement prediction error to assess whether large motion artifacts were present in the fNIRS signals. In addition, we also used the power spectrum of the efNIRS signal estimated with the Kalman filter to determine whether the efNIRS signal could be used to recognize brain activity.

The experimental results of controlling a mobile robot based on the brain activity verified that the proposed method provides better recognition of the brain activity than that without the proposed method.

In the experiments, five parameters were set at the same values for 10 subjects: the variances of 5.0×10^{-4} and 1.0×10^{-5} for w in (1) and v in (2), the threshold value of 0.4 for the measurement prediction error in (6), and the frequency of 0.07 Hz and threshold value of 2.0×10^{-4} for the power spectrum. These values were obtained from a preliminary experiment by one of authors (he was not a subject in the experiments shown in Section V). The optimal values of these parameters would depend on the subjects. In future work, we intend to improve our present abilities to detect and cancel motion artifacts by learning the optimal values of these parameters according to the subjects. In the experiments, the subjects were in 20's. Experiments by subjects from other aging ranges are also our future work.

ACKNOWLEDGMENT

This work was supported in part by the MEXT-Supported Program for the Strategic Research Foundation at Private Universities, 2014–2018, Ministry of Education, Culture, Sports, Science and Technology, Japan.

REFERENCES

[1] P. M. Arenth, J. H. Ricker, and M. T. Schultheis, "Applications of Functional Near-Infrared Spectroscopy (fNIRS) to Neurorehabilitation of Cognitive Disabilities," The Clinical Neuropsychologist, vol. 21, pp. 38–57, Jan. 2007, doi: 10.1080/13854040600878785.

[2] T. Kojima, H. Tsunashima, T. Shiozawa, H. Takada, and T. Sakai, "Measurement of Train Driver's Brain Activity by Functional Near-Infrared Spectroscopy (fNIRS)," Optical and Quantum Electronics, vol. 37, pp 1319–1338, Dec. 2005, doi:10.1007/s11082-005-4202-9.

[3] N. Naseer and K. S. Hong, "fNIRS-based Brain-Computer Interfaces: A Review," Frontiers in Human Neuroscience, vol. 9, pp.1–15, Jan. 2015, doi:10.3389/fnhum.2015.00003.

[4] M. Ferrari and V. Quaresima, "A Brief Review on the History of Human Functional Near-Infrared Spectroscopy (fNIRS) Development and Fields of Application," Neuro Image, vol. 63, pp. 921–935, Nov. 2012, doi:10.1016/j.neuroimage. 2012.03.049.

[5] Y. Hoshi, "Functional Near-Infrared Spectroscopy: Current Status and Future Prospects," J. Biomedical Optics, vol. 12:062106, Nov. 2007, doi:10.1117/1.2804911.

[6] R. J. Cooper, et al., "A Systematic Comparison of Motion Artifact Correction Techniques for Functional Near-Infrared Spectroscopy," Frontiers in Neuroscience, vol. 6, pp.1–10, Oct. 2012, doi:10.3389/fnins.2012.00147.

[7] S. Brigadoi, et al., "Motion Artifacts in Functional Near-Infrared Spectroscopy: A Comparison of Motion Correction Techniques Applied to Real Cognitive Data," Neuroimage, vol. 85, pp. 181–191, Jan. 2014, doi:10.1016/j.neuroimage.2013. 04.082.

[8] B. Molavi and G. A. Dumont, "Wavelet-based Motion Artifact Removal for Functional Near-Infrared Spectroscopy," Physiological Measurement, vol. 33, pp.259–270, Feb. 2012, doi:10.1088/0967-3334/33/2/259.

[9] M. Izzetoglu, P. Chitrapu, S. Bunce, and B. Onaral, "Motion Artifact Cancellation in NIR Spectroscopy Using Discrete Kalman Filtering," BioMedical Engineering Online, pp.9–16, March. 2010.

[10] M. Amian and S. K. Setarehdan, "Motion Artifact Reduction in fNIRS Signals by ARMA Modeling based Kalman Filtering," Int. J. Scientific Engineering Research, vol. 4, pp. 2280–2285, July 2013.

[11] T. Hiroyasu, Y. Nakamura, and H. Yokouchi, "Method for Removing Motion Artifacts from fNIRS Data Using ICA and an Acceleration Sensor," Proc. 35th Annu. Int. Conf. IEEE Engineering in Medicine and Biology Society (EMBC), pp.6800–6803, July 2013.

[12] B. Yaakov, X. Li, and T. Kirubarajan, "Estimation with Applications to Tracking and Navigation", John Wiley & Sons, Inc., 2001.

[13] T. Nakamizo, "Signal Analysis and System Identification," Corona Publishing, p. 58, 1988 (in Japanese).

[14] H. Saika, N. Miura, and S. Wang, "Recognition of Brain Activity Using Fuzzy Reasoning for NIRS-based BCI," IEICE-NC, vol.109, pp.55–58, Nov. 2009 (in Japanese).

[15] K. Takahashi, S. Maekawa, and M. Hashimoto, "Remarks on Fuzzy Reasoning-based Brain Activity Recognition with a Compact Near Infrared Spectroscopy Device and its Application to Robot Control Interface," Proc. Int. Conf. Control, Decision and Information Technologies (CoDIT), pp.615–620, Dec. 2014, doi:10.1109/CoDIT.2014.6996966.